Three-dimensional reconstruction of individual cervical vertebrae from cone-beam computed-tomography images

Hongjian Shi,[a] William C. Scarfe,[b] and Allan G. Farman[c]
Louisville, Ky

Introduction: The visualization of cervical vertebral morphology has potential in skeletal age assessment; however, thus far, it has only been described in planar images. The objective of this article is to present a novel segmentation algorithm for automatic 3-dimensional (3D) reconstruction of individual cervical vertebrae from cone-beam computed-tomography (CBCT) volumetric data sets. **Methods:** CBCT data sets of 3 subjects representing different skeletal age groups with no potential health influences on cervical anatomy were identified from a larger subject sample. A visualization toolkit was used to demonstrate the surface topologic shape of cervical vertebrae C1 through C3. The cervical vertebrae were segmented by using a custom algorithm based on individual voxel intensity distribution analysis and propagation from a densitometric start point to generate the whole vertebra. The segmentation algorithm was combined with toolkit visualization to render and save the cervical vertebra in 3D space. **Results:** The developed segmentation algorithm separated individual cervical vertebrae successfully. It was robust and efficient. Observed 3D cervical vertebral morphologic features from the 3 examples matched the known 2-dimensional sagittal shape changes of the cervical vertebra with respect to subject age and skeletal maturation. **Conclusions:** Segmentation of individual vertebrae proved possible from CBCT volumetric data sets. This provides a 3D approach to the biologic aging of orthodontic patients by using images of the cervical spine. It also has potential in studying disease processes such as spinal fractures consequent to osteoporosis. (Am J Orthod Dentofacial Orthop 2007;131:426-32)

Cervical vertebral maturation is significantly related to skeletal maturation and can be used to predict skeletal age, a useful input in determining growth potential for planning orthodontic treatment.[1-5] O'Reilly and Yaniello[6] specifically assessed the relationship of cervical vertebral maturation to mandibular growth changes, whereas Mito et al[7] introduced a regression formula to determine skeletal maturation from cervical vertebral morphology. Evaluation of cervical vertebral morphology and related maturation assessment has proven successful in correct diagnosis and treatment planning in relation to human growth and development.[4,5,8]

Previous studies on the relationship of cervical vertebral maturation to skeletal maturation focused on the shape changes of cervical vertebrae C1, C2, and C3 profiles observed in the sagittal plane by using standard lateral cephalograms.[1-5] The shape changes in 2-dimensional (2D) sagittal views were described in 6 stages: initiation, acceleration, transition, deceleration, maturation, and completion.[2,4,5,8] Farman[8] detailed 2D shape changes of individual C3 vertebrae in sagittal views with increasing biologic age and commented on a discrepancy between males and females in maturation through 19 years; girls were slightly ahead of boys up to that chronologic age. Two-dimensional sagittal views provide a good reference to observe the shape changes of cervical vertebrae in various growing periods; however, cone-beam computed tomography (CBCT) adds a potentially useful third dimension.

The purpose of this technical report was to present a feasibility study of an automatic segmentation algorithm to separate individual cervical vertebrae from CBCT volumetric data sets and to visualize them in 3 dimensions.

MATERIAL AND METHODS

With institutional review board approval, 3 representative anonymous CBCT data sets from patients aged 9, 17, and 27 years were selected to represent

From the Division of Radiology and Imaging Science, Department of Surgical and Hospital Dentistry, University of Louisville, Louisville, Ky.
[a]Research associate.
[b]Associate professor.
[c]Professor.
Reprint requests to: Allan G. Farman, Department of Surgical and Hospital Dentistry, University of Louisville, 501 S Preston St, Louisville, KY 40292; e-mail, agfarm01@louisville.edu.
Submitted, October 2005; revised and accepted, December 2005.
0889-5406/$32.00

doi:10.1016/j.ajodo.2005.12.031

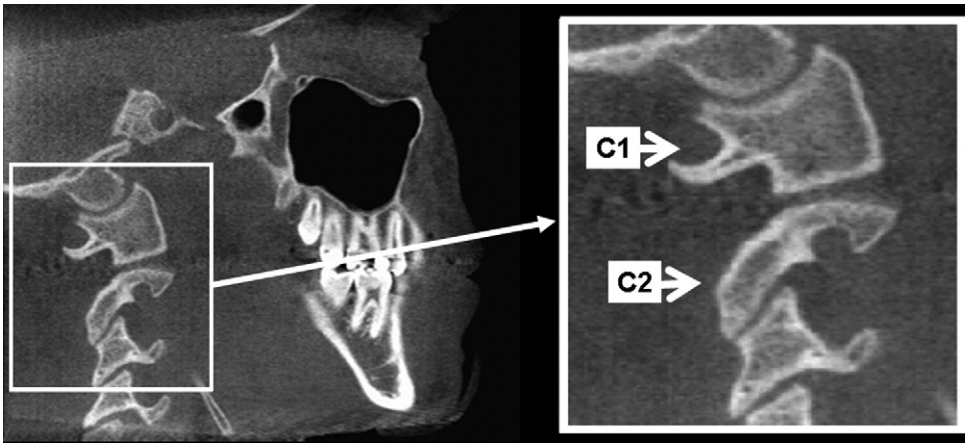

Fig 1. *Left,* Sagittal view from stack of CBCT images shows cervical vertebrae C1, C2, and C3. *Right,* Portion of zoomed sagittal view contains cervical vertebrae C1, C2, and C3 and shows separation of vertebral segments by interarticular soft tissue.

different growth periods. Fifty other anonymous data sets were also examined to determine common geometric features of the cervical vertebrae. These data sets had been acquired for various purposes unrelated to the cervical spine. The selected data sets contained complete images of cervical vertebrae C1, C2, and C3.

Sixteen-bit DICOM images were reduced to 8-bit JPEG to develop the segmentation algorithm. The algorithm was based on common geometric features of cervical vertebrae observed from 50 CBCT images. For most subjects, each cervical vertebra was separated from its immediate neighboring superior and inferior cervical vertebrae by intervertebral discs. The intervertebral discs had similar beam attenuation to the other soft tissues, with the cervical vertebral bone clearly higher in beam attenuation intensity values. This difference in resulting radiodensity can be observed from the 2D sagittal CBCT image detail (Fig 1).

In our formulation of the segmentation algorithm, a coordinate system was selected so that the "length" of transaxial slices was the x-axis with the positive direction pointing to the right. The "width" was the y-axis with the positive direction pointing downward. The "height" of the stack of slices was the z-axis with the positive direction pointing to the largest slice number.

To separate a cervical vertebra from the rest of the image, a point O was designated as a starting (reference) point belonging to the cervical vertebra to be segmented. Figure 2 shows a pixel board of the zoomed versions of partial C2 and partial C3 in 2D. The pixel intensity values in the bony region of the cervical vertebra were relatively high compared with those of neighboring soft tissues. From the proprietary imaging software provided for CBCT image analysis (i-CAT, Imaging Sciences International, Hatfield, Pa), the location and intensity of the reference point O was readily determined. Starting from the reference point, the 6 immediately neighboring voxels were examined: left, above, right, and below voxels in the same slice with the reference point O, and the 2 nearest points in the immediately adjacent superior and inferior slices. The algorithm principle applied to the 3-dimensional (3D) object was the same as for a 2D object except that the reference had 2 more neighboring points. For example, the points that could be identified as belonging to C3 were determined first. The selected point O in Figure 2 belongs to C3 but is close to the boundary with C2; each has an intensity value larger than a determined threshold. Between 2 neighboring cervical vertebrae, there is an intervertebral disc that has, in most instances, a relatively low beam attenuation intensity compared with the 2 neighboring cervical vertebrae. On, or near, the boundary of the cervical vertebrae and the intervertebral disc, points usually had gradient vectors of relatively high magnitude, so it was possible to find a threshold gradient vector magnitude to determine whether a point belonged to the cervical vertebra or the intervertebral disc. To classify a point as cervical vertebra, 2 thresholds were used as components for the proposed segmentation algorithm. One was the approximate lower bound of the intensity values of the cervical vertebra, and the other was the approximate upper bound of the gradient vector magnitudes from the selected points of the cervical vertebra compared with its neighboring points.

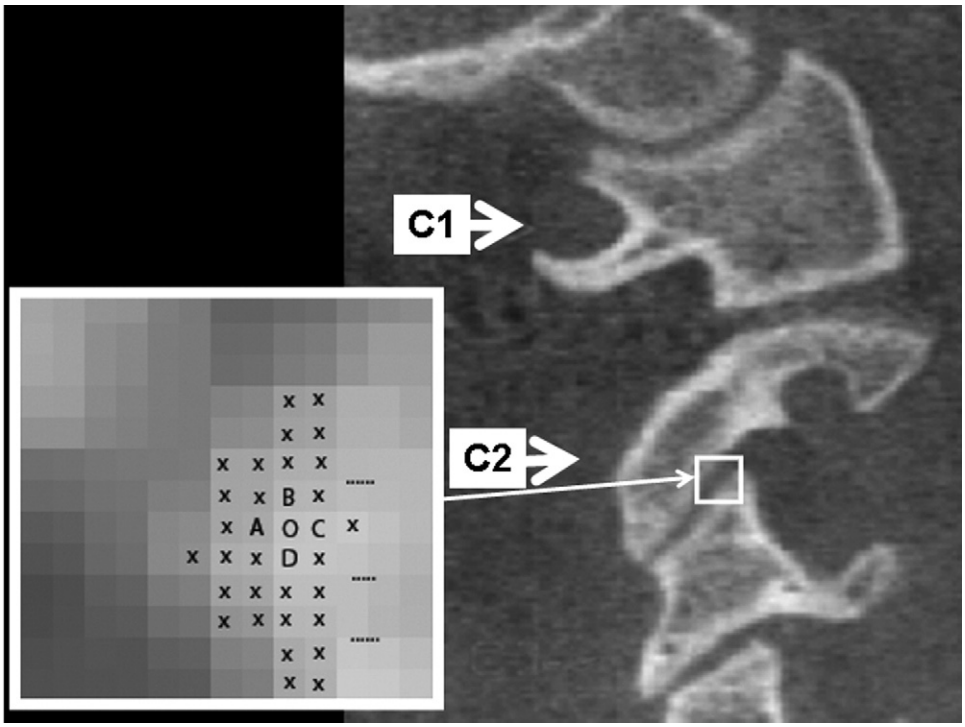

Fig 2. Segmentation algorithm illustration shows start point O (reference point) and propagation to individual cervical vertebra. A (*left*), B (*above*), C (*right*), and D (*below*) are 4 immediate neighboring points to reference point O.

For illustration, the intensity threshold for C3 in Figure 2 was set to 160 (from a grayscale pixel value range of 0 to 255). The threshold of the gradient vector magnitudes was set to 30. The selected reference point O belonged to vertebral bone and had an intensity value of 205. Then, this intensity value (205) was set to 255 and marked as the selected point. Four neighboring points, A, B, C, and D, were then classified. Point A had an intensity value of 185 (ie, larger than the set intensity threshold of 160), and the gradient magnitude difference from O to A was 20 (ie, less than the gradient vector magnitude 30). So, point A was classified as a point within the cervical vertebra C3 and was marked as a selected point. Points B, C, and D were also classified as points on the cervical vertebra C3 in the same manner. It was then necessary to classify the points neighboring point A. Point O was a neighboring point but was already selected and did not need to be verified again. The examination order for the neighboring points of A was clockwise. This process continued until a point was encountered that was verified as belonging to the bone of the cervical vertebra for which neighboring points were already selected as belonging or not belonging to cervical vertebra C3. Selected points (marked X) on the boundary region of C3 and the intervertebral disc show clear separation of C3 from C2 when the propagation method was used to separate C3 from the rest of the image (Fig 2).

The algorithm is similarly applied to 3D data sets but incorporates 2 more neighboring points in the immediately superior and inferior slices. The 2 thresholds were not fixed at the beginning. They can be changed from 1 cervical vertebra to another and can be found by trial and error. The intensity threshold was found in the pixel value range of 140 to 180, and the gradient vector magnitude threshold was found in the pixel value range of 9 to 40. Usually, trial and error was required 3 to 5 times until a desired 3D cervical vertebra was obtained. Obviously, if the cervical vertebra can be separated with a smaller bone intensity threshold and a larger gradient magnitude threshold, the segmentation result will be better in keeping the entire shape of the cervical vertebra. This is particularly the case for high-curvature regions. To separate an individual cervical vertebra, sometimes the intensity threshold had to be raised, and the gradient magnitude threshold had to be reduced. Higher or lower thresholds did

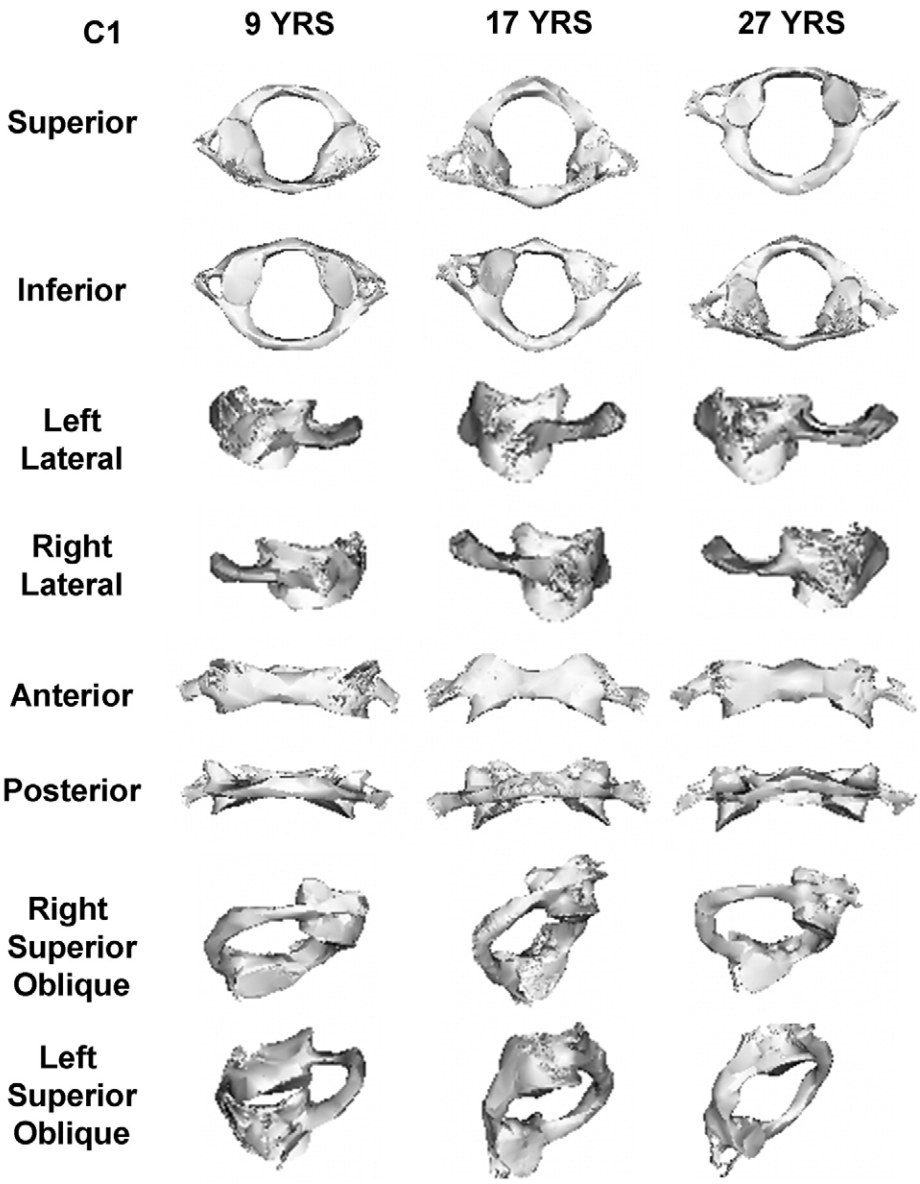

Fig 3. Bilateral sagittal, anterior and posterior coronal, superior and inferior axial, and left and right lateral oblique projections of cervical vertebrae C1 of subjects aged 9, 17, and 27 years, respectively.

not affect the shape of the object, because the 2 thresholds were uniform for each vertebra. Nonetheless, the chosen thresholds might affect the size of the target object slightly because of the inclusion or removal of boundary points when the thresholds are very high or very low.

Rarely, 1 cervical vertebra was apparently connected directly with another cervical vertebra resembling osseous fusion. In our 50 reference test subjects, only 1 had apparent bony fusion. This could have been actual or an artifact if the thickness of the intervertebral disc between C2 and C3 is less than, or equal to, the selected voxel resolution (0.4 mm in our study). In this 1 case, the algorithm could not distinguish the boundaries of the adjacent C2 and C3 vertebrae.

Because the left, right, and posterior components of cervical vertebrae have convexities and concavities, segmentation might result in some loss. This cannot be avoided because the separation between 2 neighboring cervical vertebrae needs a threshold of the gradient vector magnitudes.

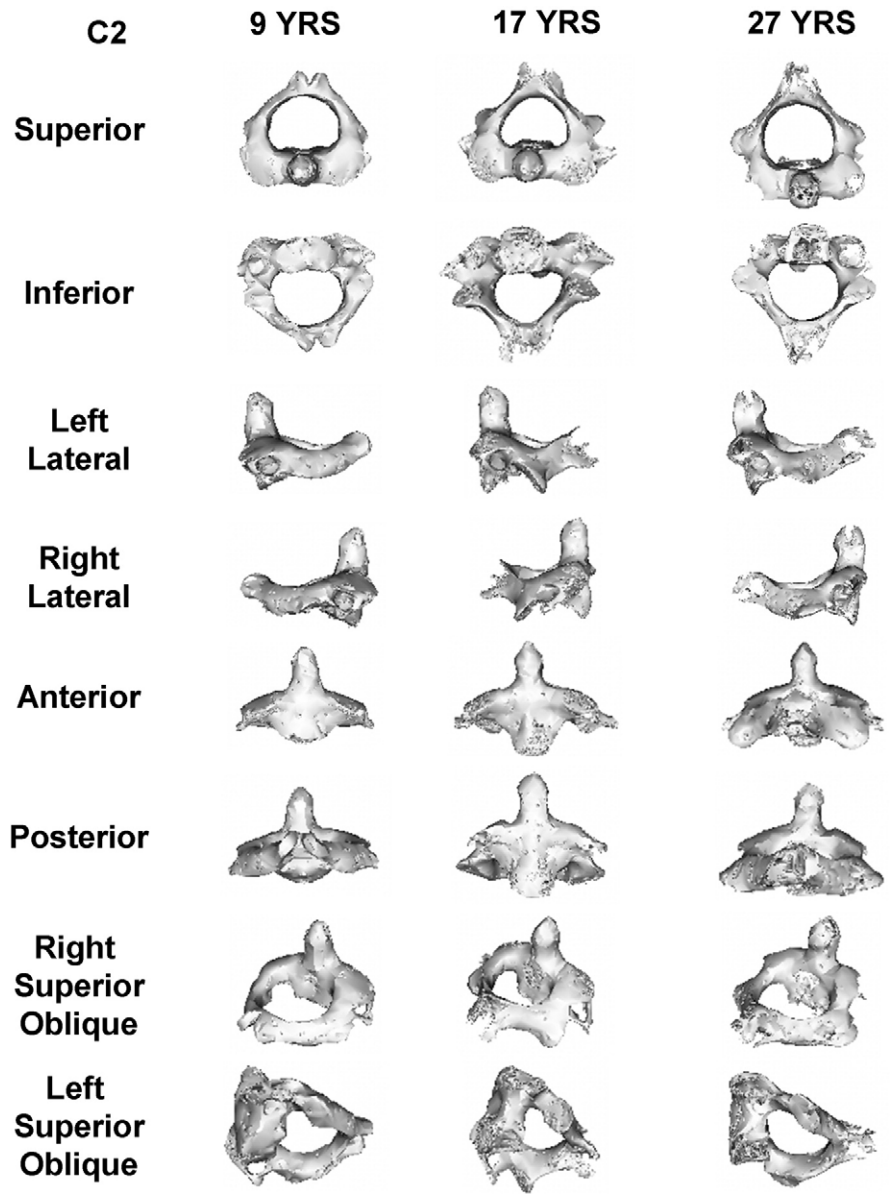

Fig 4. Bilateral sagittal, anterior and posterior coronal, superior and inferior axial, and left and right lateral oblique projections of cervical vertebrae C2 of subjects aged 9, 17, and 27 years, respectively.

RESULTS

Figure 3 shows multiple orientations of C1 for subjects aged 9, 17, and 27 years, respectively. These views indicate that with increasing age the supero-inferior posterior arch curvature becomes more acute with a resultant apparent increase in length and superior rotation. In addition, it is observed that the 2 sides on the left and right components extend superiorly and inferiorly, leaving the middle portion relatively thinner with increased age.

Figure 4 shows multiple orientation projections of C2 for subjects aged 9, 17, and 27 years, respectively. Similar to C1, the distal tubercle of C2 appears to rotate superiorly with increasing age. In addition, the lower surface of the anterior arch of the cervical vertebra appears to become flatter, whereas the superior surface of the anterior arch becomes more prominent with increasing age.

Figure 5 shows multiple orientations of C3 for subjects aged 9, 17, and 27 years, respectively. With

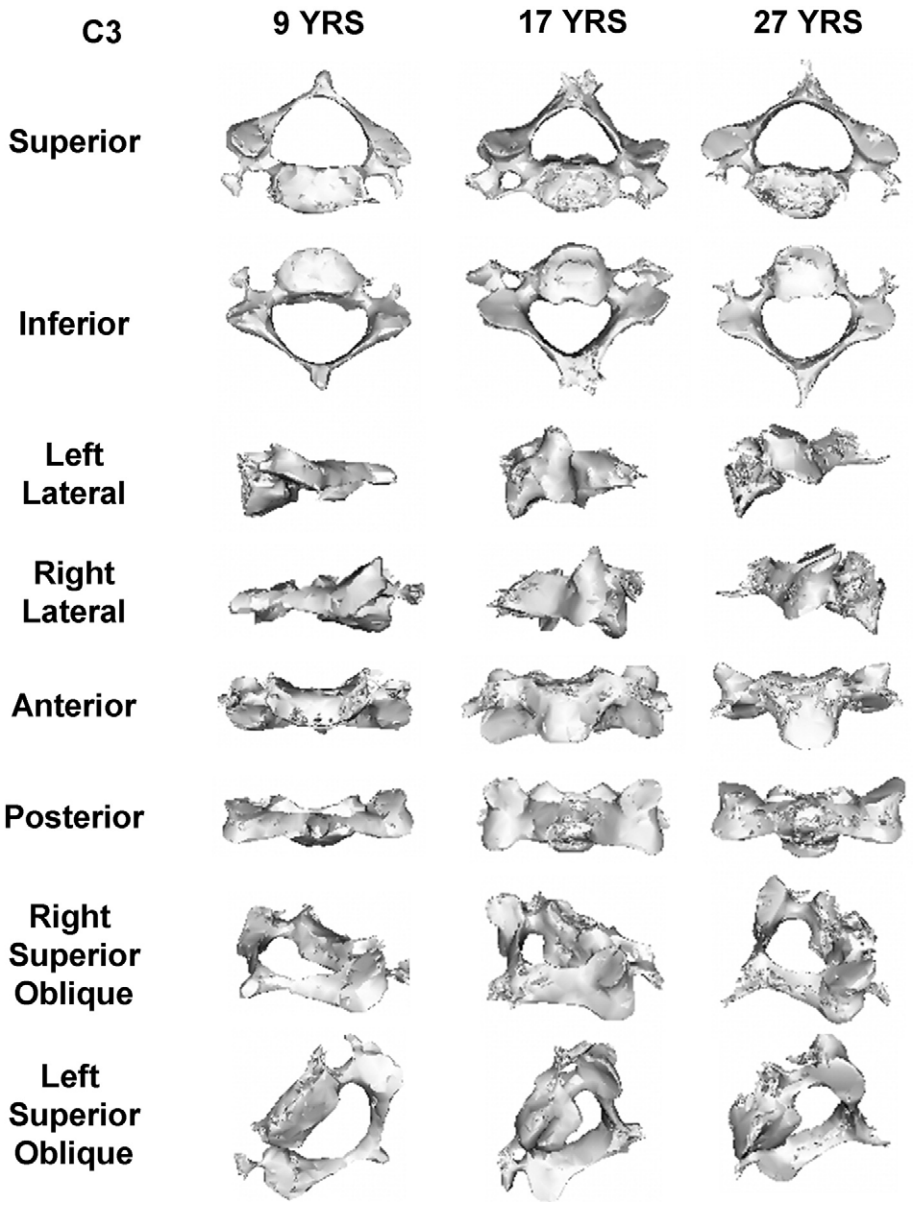

Fig 5. Bilateral sagittal, anterior and posterior coronal, superior and inferior axial, and left and right lateral oblique projections of cervical vertebrae C2 of subjects aged 9, 17, and 27 years, respectively.

increasing age, it appears that the inferior surface of the anterior tubercle becomes more prominent and convex anteriorly, whereas the superior surface becomes upwardly concave.

DISCUSSION

The 3D findings in this technical feasibility study closely matched the observation by Hassel and Farman.[2] When viewed anteriorly, the lower surface of the anterior portion of each cervical vertebra becomes more prominent with increasing age. These features can also be observed in ray-sum simulations of lateral cephalometric radiographs from the 3 subjects we studied (Fig 6). These 2D reformations are generated by creating a sagittal plane through the middle of the cervical data set and representing all available voxels to a selected thickness, in this case 100 mm. Further validation of the utility of the proposed algorithm for vertebral segmentation in skeletal age determination is needed using a larger

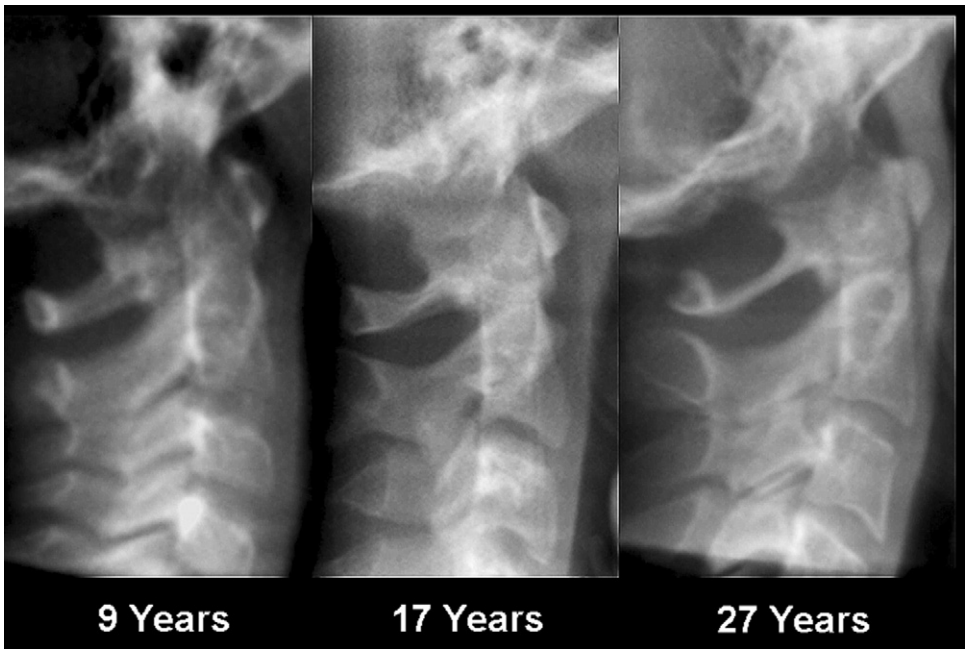

Fig 6. Ray-sum simulations of cervical vertebrae from CBCT data sets of lateral cephalograms for subjects aged 9, 17, and 27 years, respectively.

study population and prospective evaluation of morphologic changes over time.

We must make certain caveats concerning this study. Threshold levels were arrived at by trial and error. The effect of threshold levels on the final shape and extent of each vertebra was not assessed objectively. A future objective assessment should include counting the number of voxels assigned to each vertebra for each threshold level. Furthermore, this study involved the conversion of 16-bit DICOM image files to 8-bit JPEG. Adjustment of the algorithm to directly use the original DICOM image files would improve the integrity of the original image data and associated information tags. The selection of JPEG files with reduced dynamic range was to simplify developing and testing the algorithmic approach during this feasibility study.

CONCLUSIONS

Segmentation of individual vertebrae proved possible from CBCT volumetric data sets. The results of this 3D pilot study matched well with previous reports in the literature concerning shape changes with skeletal age as judged in 2D sagittal views. This provides a possible 3D approach to the biologic aging of orthodontic patients by using images of the cervical spine. It also has potential in studying disease processes such as spinal fractures consequent to osteoporosis.

REFERENCES

1. Lamparski D. Skeletal age assessment utilizing cervical vertebrae (thesis). Pittsburgh: University of Pittsburgh; 1972.
2. Hassel B, Farman AG. Skeletal maturation evaluation using cervical vertebrae. Am J Orthod Dentofacial Orthop 1995;107:58-66.
3. Garcia-Fernandez P, Torre H, Flores L, Rea J. The cervical vertebrae as maturation indicators. J Clin Orthod 1998;32:221-5.
4. Román PS, Palma JC, Oteo MD, Nevado E. Skeletal maturation determined by cervical vertebrae development. Eur J Orthod 2002;24:303-11.
5. Baccetti T, Franchi L, McNamara JA Jr. An improved version of the cervical vertebral maturation (CVM) method for the assessment of mandibular growth. Angle Orthod 2002;72:316-23.
6. O'Reilly MT, Yanniello GJ. Mandibular growth changes and maturation of cervical vertebrae—a longitudinal cephalometric study. Angle Orthod 1988;58:179-84.
7. Mito T, Sato K, Mitani H. Cervical vertebral bone age in girls. Am J Orthod Dentofacial Orthop 2002;122:380-5.
8. Farman AG. Assessing growth and development with panoramic radiographs and cephalometric attachments: a critical tool for dental diagnosis and treatment planning. Panoramic Imaging News 2004;4(4):1-12.